QIRT 10
http://dx.doi.org/10.21611/qirt.2010.102
10th International Conference on Quantitative InfraRed Thermography
July 27-30, 2010, Québec (Canada)

Region of Interest Extraction based on Multi–resolution Analysis for Infrared Nondestructive Testing

by B. Ortiz-Jaramillo*, H. Benitez-Restrepo**, J. Garcia-Álvarez* and G.Castellanos-Dominguez*

** G. Procesamiento y Reconocimiento Señales, Universidad Nacional de Colombia, Manizales, bortizj@unal.edu.co*
*** G. DESTINO Pontificia Universidad Javeriana de Cali, hbenitez@javerianacali.com*

Abstract

In this paper, a methodology for ROI extraction in INDT using multi-resolution analysis is proposed. Complementary, both local procedures Harris operator and gradient direction are used. The proposed methodology is tested using three CFRP specimens having complex shapes and defects at different depths. Besides, another two specimens are considered, which are made of PlexiglasTM and aluminum with circular flat bottom holes at different depths. The results show that the proposed methodology is invariant to the material or defect shape among considered plates, moreover the methodology only has two parameters with no dependency of the variable features of the inspected object.

1. Introduction

The ultimate goal of a thermographic inspection is to automatically analyze images providing a pass or fail diagnostic to the operator. In this line of analysis, pulse infrared thermography that is known as an effective and rapid method of nondestructive inspection can be applied to detect a broad range of near-surface structuring flaws in metallic and composite components, such as disbonds, delaminations, corrosion and fatigue cracks, and requires only single-sided access to the subject. Dedicated algorithms of thermographic inspection must detect the presence of defects, termed as Regions of Interest (ROI), over images that are characterized by low contrast. Specifically, thermal diffusion is modeled as a smooth contour centered at a peak of stored thermal energy, which may represent regions in materials with potential anomalies or failures. For this reason, Gaussian model is one of the most used heat flow descriptor since it achieves proper results in approximating heat diffusion processes [1]. Due to the Gaussian nature of the ROI, thermal image can be characterized as localized contrast image, i.e., the image uses the entire range of the histogram, but each ROI has a very low contrast. Thus, peaks located on Gaussian heat surfaces are hard to detect [2]. In this sense, the primary difficulty in making useful interpretations of a thermal image is the presence of thermal noise, optical distortion through the thermal imaging system, and of most concern, non-uniform heating caused by the uneven excitation of the surface. Moreover, non-uniform heating is difficult to remove since it establishes an aberration that varies in time. Since this effect varies from image to image, a simple reference subtraction is not convenient [3]. In summary, Region growing approach for image segmentation in Infrared Nondestructive Testing (INDT) is affected by ROI low contrast and non-uniform heating.

Previous works in INDT have faced above explained restrictions. Thus, in [4], it is proposed an automatic segmentation method for steel strips, where segmentation is made using gradient operators to define boundaries of each region. Nonetheless, tuning of parameters such a segmentation threshold, operator size and projection value is to be strongly considered. In [5], an automatic segmentation algorithm is proposed based on the relatively low spatial content of structures over the INDT infrared images. In this algorithm, seeds are first reliably located grounded on a global sorting process within the entire image. Then, for each region, a threshold is found by means of a region growing approach, which starts at the central point of a detected defect and stops when either an image border is hit or the number of pixels agglomerated together around the seed increases abruptly. Nevertheless, to get effective results with this algorithm, parameters such minimum neighbor distance (MND) and number of defects must be established by trial and error, and that task is far to be easy implemented. Besides, stop criteria of region growing is affected by non-uniform heating. In [6], it is presented an automatic detection algorithm of subsurface defects for a concrete case of bridge decks using infrared thermography. In this work, the segmentation algorithm starts with the hottest pixels found thorough the image, which further are labeled as seed points; then, regions are grown around them based on any given neighborhood selection criterion. Although, the achieved performance is not measured by any metrics, the introduced assumption that centers of defect areas are those pixels with the highest gray level may be not always true because of non-uniform heating phenomena. In [2], another technique is proposed for segmenting defects in a thermal image of petrochemical equipments acquired by passive thermography. The technique firstly enhances the contrast of the defects based on intensity operations in local neighborhood pixel. Then image is segmented by histogram thresholding. Even that achieved results seem to be adequate, contrast enhancement technique uses regular block sizes, which is not necessary the case if being affected by non-uniform heating. Generally, previous considered works require to fix beforehand parameters that are related just with the object to be inspected, and therefore

restricting proposed algorithms to specific applications such as inspections of steel, concrete bridge decks or petrochemical equipments and fails when they are tested with different materials and defect types.

In this paper, a methodology for ROI extraction in INDT using multi-resolution analysis and redundant wavelet transform is proposed, which should be robust to non-uniform heating since multi-resolution analysis provides enough scale information. Complementary, both local procedures Harris operator and gradient direction are used since they are not affected by other structures in the thermal image. Former procedure is used to detect local maxima (seeds in region growing), while gradient direction is introduced for region growing. In addition, this methodology only requires the adjustment of wavelet decomposition level and structuring element size, which depends on thermal image features, but not on the variable features of the inspected object. The paper is organized as follows: in Section 2 a brief explanation is given about redundant wavelet transform, Harris operator, region growing following the gradient direction. Detailed description of used algorithm provided. Section 3 describes the experimental procedure, including the achieved comparison among the proposed methodology with another state-of-the-art procedures. Besides the best combination between levels of decomposition and structuring element to achieve the best performance is carried out. Section 4 carries out the discuss of the results by applying the proposed methodology, and finally conclusions are provided.

2. MATERIALS AND METHODS

2.1. Redundant Wavelet Transform and Multi-scale Gradient Approximation

Let $\mathbf{C} \in ¡^{M \times N \times Q}$ be an array of wavelet coefficients that describes an image $\mathbf{X} \in ¡^{M \times N}$, being M the number of rows, N the number of columns, and $Q = 2^L + 2$, with L the chosen number of levels in wavelet decomposition, where a wavelet function $\phi(\cdot)$ is introduced for representing the set of different P ROI, $\mathbf{\Omega}_p \in ¡^{H \times W}$, $p = 1...P$, $1 \le H \le M$, $1 \le W \le N$ under the restriction that the given function must have less than 2 vanishing moments to provide detail coefficients that take the energy of the borders, i.e., wavelet detail coefficients should have maximum modules at borders of $\mathbf{\Omega}_p$. In this work, selection of Haar mother wavelet (having 1 vanishing moment) is suggested since attained components of detail become closer to the image gradient, that is, given a wavelet high pass filter $\mathbf{h} = [-(2)^{-1/2} \ (2)^{-1/2}]$, as well as an one-dimensional signal $\mathbf{x} = \{x_i : i \in ¥\}$, their convolution yields $\mathbf{y} = \mathbf{x} * \mathbf{h}$ and therefore, $y_i = (x_i - x_{i-1}) / 2^{1/2} = \Delta x / (2^{1/2} \Delta i)$, thus, $\mathbf{y} \approx d\mathbf{x} / di$. If extending this approach to two-dimensional signals and using the pyramidal algorithm [7], it follows that: $y^1_{i,j} = x_{i,j} - x_{i,j-1} / (2^{1/2} \Delta j)$ and $y^2_{i,j} = x_{i,j} - x_{i-1,j} / (2^{1/2} \Delta i)$, then $\mathbf{Y}_1 = \Delta \mathbf{X} / \Delta j$ and $\mathbf{Y}_2 = \Delta \mathbf{X} / \Delta i$. As a result, $\mathbf{Y} = [\mathbf{Y}_1 \ \mathbf{Y}_2]^T \approx \nabla \mathbf{X}$, i.e., the components of horizontal and vertical details of wavelet transform using Haar mother wavelet are close to gradient of $\mathbf{X}$.

When scale is reduced, for each decomposition level, irrelevant details are lost and only those that provide information are preserved (termed hot spots). Thus, the accumulated wavelet module is defined, $\mathbf{\Delta}_\Sigma = \sum_{j=1}^{L} \mathbf{\Delta}_j$, where L is the maximum level of decomposition, and $\mathbf{\Delta}_j = \sqrt{\mathbf{D}^2_{j,1} + \mathbf{D}^2_{j,2} + \mathbf{D}^2_{j,3}}$, $\mathbf{D}_{j,i} \in ¡^{M \times N}$, with $\mathbf{D}_{j,1}$, $\mathbf{D}_{j,2}$, and $\mathbf{D}_{j,3}$ the detail coefficient in scale j in horizontal, vertical, and diagonal directions respectively. Thus, a relevant peak detected by wavelet transform can be preserved through scale reduction. Moreover, the higher accumulated wavelet module, the more relevant all local maxima. Then, the gradient method is used to find the size of the region from the initial position of local maxima. Specifically, detection of each ROI is carried out based on the local maxima approach, proposed in [7].

In order to reduce the processing time an interest point can be extracted from $\mathbf{\Delta}_\Sigma$ by simple thresholding, in particular, by means of the Harris operator, since it does not require any threshold adjustment.

Due to the fact that wavelet transform coefficients, $\mathbf{A}_L$ and $\mathbf{D}_{j,o}$, are sub-sampled, a redundant scheme is required to preserve original image scale. To cope with this shortage, the redundant discrete wavelet transform (RDWT), which had been proposed [8] for signal detection and enhancement, is achieved, since it preserves uniform sampling rate in space domain and also is a discrete approximation to the continuous wavelet transform [9]. Besides, RDWT is shift invariant and its redundancy introduces a complete expansion that in turn increases the robustness to additive noise, i. e., addition of noise in wavelet coefficients leads to less signal distortion than the discrete wavelet transform (DWT) expansions [8, 9]. Moreover, redundant wavelet transform removes the decimation operators from DWT filter banks, as shown in Figure 1.

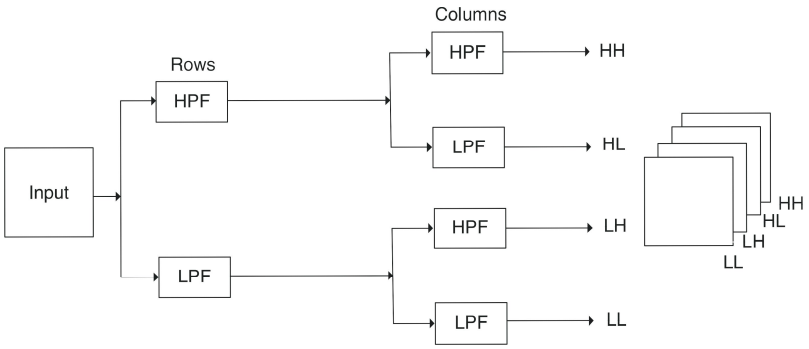

Fig. 1. *Redundant Wavelet Transform*

Nevertheless, the wavelet filters must be adjusted accordingly at each scale. Thus, $h_1[k] = h[k]$, where $h_1[k]$ is the RDWT low pass filter at scale 1 and $h[k]$ is DWT scaling filter. Filters at later scales are up-sampled versions from the filter coefficients at the upper state, $h_{l+1}[k] = h_l[k] \uparrow 2$ and similar definitions are applied to high pass filter $g_l[k]$ [9]. Another method used is "Á Trous Algorithm" that approximates the values at non-integral points through interpolation via a finite filter [8]. The resulting recursion is highly efficient and is implemented with the filter bank structure, as shown in Figure 1 [9].

2.2. Harris Operator-based Analysis

As stated above, interest points can be detected if local maxima is calculated, by estimating Δ_Σ, it represents local features where signal changes in both dimensions; in general, they have high information content [10]. In this line, a considerable variation can be fixed if the weighted sum of square difference is computed between the original image $\mathbf{X}$ and its shifted version on (i, j) positions:

$$\begin{aligned} \mathbf{S}(i, j) &= \sum_{m\in b}\sum_{n\in b} w(m,n)\big(\mathbf{X}(m,n) - \mathbf{X}(m+i, n+j)\big)^2 \\ &\approx \sum_{m\in b}\sum_{n\in b} w(m,n)\big(j\mathbf{X}_1(m,n) + i\mathbf{X}_2(m,n)\big)^2 \end{aligned} \quad (1)$$

where $\mathbf{X}_1$ and $\mathbf{X}_2$ are the partial differences of $\mathbf{X}$, such that $\mathbf{X}(m+i, n+j) = \mathbf{X}(m,n) + j\mathbf{X}_1(m,n) + i\mathbf{X}_2(m,n)$. Besides, as square weighting matrix $w(m,n) \in ¡^{b\times b}$ a Gaussian function is used. Equation 1 can be expressed in matrix form, $\mathbf{S}(i, j) = [i\ j]\mathbf{A}[i\ j]^T$, where $\mathbf{A}$ is the Harris operator, that describes the gradient distribution in a given neighborhood, defined by the following tensor structure matrix:

$$\mathbf{A} = \begin{bmatrix} \mathrm{E}\{\mathbf{X}_1^2\} & \mathrm{E}\{\mathbf{X}_1\mathbf{X}_2\} \\ \mathrm{E}\{\mathbf{X}_1\mathbf{X}_2\} & \mathrm{E}\{\mathbf{X}_2^2\} \end{bmatrix} \quad (2)$$

here, $\mathrm{E}\{\cdot\}$ stands for the expectation operator.

Therefore, any interest point is characterized by considerable variation of $\mathbf{S}$ in all directions of vector $[i, j]$. Let λ_1 and λ_2 be the eigenvalues of $\mathbf{A}$. Then, based on the magnitude of the eigenvalues, it can be inferred that [11]:

— If $\lambda_1 \approx 0$ and $\lambda_2 \approx 0$, then the pixel $[i, j]$ is not an interest feature.

http://dx.doi.org/10.21611/qirt.2010.102
10th International Conference on Quantitative InfraRed Thermography

— If $\lambda_1 \approx 0$ and λ_2 has some large positive value, then an edge is found.

— If λ_1 and λ_2 have large positive values, then a corner is found.

The attained maxima Δ_Σ can be viewed as a corner because their values present changes in all directions, i.e., they can be detected by using the Harris operator and to be selected as interest point. The general procedure of the multi-resolution ROI extraction is shown in Algorithm 1.

Algorithm 1 Methodology of segmentation

INPUTS
Gray scale image $\mathbf{X}$
OUTPUTS
Binary image $\mathbf{BW}$
Calculate coefficients $\mathbf{C}$ of the wavelet transform with L levels of decomposition
Compute wavelet modulus Δ_j for each scale j and calculate Δ_Σ.
Calculate the direction in the first level of decomposition Δ_1.
Get the tensor $\mathbf{A}$ and choice P points that meets the criteria described by eigenvalue analysis.
FOR $p = 1$ **until** P
Size of $p-th$ region $\gamma = 0$
WHILE $\Delta_\Sigma(\mathbf{k}) \geq \Delta_\Sigma(\mathbf{k} \pm \mathbf{v})$
$\gamma = \gamma + 1$
$\mathbf{k} = \mathbf{k} + \mathbf{v}$
ENDWHILE
$\mathbf{\Omega}_p = square(i, j, \gamma)$ {Generate square with size γ and initial pos (i,j)}
ENDFOR

$$\mathbf{BW} = \begin{cases} 1 \text{ if } (i,j) \in \mathbf{\Omega}_p \forall p \\ 0 \text{ otherwise} \end{cases}$$

In Algorithm 1 the gradient is defined as:

$$\angle\mathbf{\Delta}_1(\mathbf{k}) = \begin{cases} \arctan\left(\mathbf{D}_{1,2}(\mathbf{k}) / \mathbf{D}_{1,1}(\mathbf{k})\right), & \mathbf{D}_{1,1}(\mathbf{k}) \geq 0 \\ \pi - \arctan\left(\mathbf{D}_{1,2}(\mathbf{k}) / \mathbf{D}_{1,1}(\mathbf{k})\right), & \text{otherwise} \end{cases} \quad (3)$$

and the displacing vector $\mathbf{v} \in \{(1,0),(0,1),(1,1),(1,-1)\}$ is chosen to be close to the vector $(-\sin(\angle\mathbf{\Delta}_1(\mathbf{k})), \cos(\angle\mathbf{\Delta}_1(\mathbf{k})))$, being orthogonal to local edge direction.

3. EXPERIMENTAL SET-UP

Figure 2 shows the proposed methodology of ROI extraction based on multi-resolution features, extracted from wavelet representation space. The methodology, used for infrared nondestructive testing, comprises the following stages: a) Pre-processing, b) Feature extraction using redundant wavelet transform, and including the estimation of point of interest by Harris operator, c) Post-processing and d) Evaluation.

3.1. Database and Preprocessing

http://dx.doi.org/10.21611/qirt.2010.102

The proposed methodology is tested using three CFRP (Carbon Fiber Reinforced Plastic) specimens (namely, *CFRP006*, *CFRP007*, and *CFRP008*) having complex shapes, defects at different depths, and with different sizes. Besides, another two

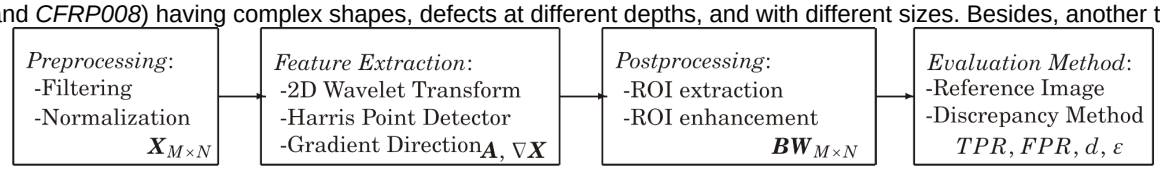

Fig. 2. *Diagram of proposed ROI extraction methodology based on wavelet representation space*

specimens are considered, which are made of PlexiglasTM and aluminum with circular flat bottom holes at different depths [12]. Experimental testing is performed using two flash lamps (Balcar *FX 60*, *6.4 kJ*), with a 5 ms pulse, as excitation source. All the thermogram sequences were recorded using a FPA infrared camera (Santa Barbara Focalplane *SBF125*, 3 to 5 μm), with a 320x256 pixel array. The number of frames, the frame size and the sampling period Δt of each sequence are listed in Table [12].

The preprocessing stage comprises both the filtering process and the normalization process. Gaussian filtering is used for simplicity of implementation and rotationally symmetric property [13,14] which is devoted to reduce background noise that corrupts each frame. Once the filtering stage is carried out, the normalization procedure of the frames, which is needed to provide independence in the sense of main image properties such as brightness and contrast, is achieved by, $\mathbf{X}' = (\mathbf{X} - \mu_{\mathbf{X}}) / \sigma_{\mathbf{X}}$, where $\mu_{\mathbf{X}}$ is the mean value and $\sigma_{\mathbf{X}}$ is the standard deviation of the filtered image.

3.2. Feature Extraction

As main issues, when using infrared nondestructive testing image analysis, the non-uniform heating and low contrast in ROI (say defects) are referred. Since non-uniform heating has influence on low spatial frequency regions [3], it might be suggested that a high pass filtering would reduce the non-uniform heating effect, even its inclusion increases the high frequency noise not filtered during the pre-processing stage. Scale information provided by wavelet multi-resolution analysis aids to overcome this shortage, because the use of wavelet transform splits non uniform heating from relevant details in the image, without increasing high frequency noise. In this sense, Haar filter is used to this purpose since Wavelet transform is close to image gradient at different resolutions, according to the piramidal algorithm [7].

Furthermore, accumulated wavelet module, $\mathbf{\Delta}_{\Sigma}$, provides information to detect objects of interest (defects) in the case of thermal images, but not their positions, which can be estimated by using the Harris operator that is given by Equation 2. Once the points of interest are calculated, the gradient direction is used to appraise the ROI size starting from the point of interest and following the gradient direction. The ROI border is fixed at the location where gradient magnitude abruptly changes.

One of the algorithm parameters, the wavelet level is set by the assumptions in [15], therefore, the edge is localized using a neighborhood analysis having a size proportional to the size of the blur, i.e, proportional to the smoothing size of the edge, when $L = k\sigma$, where k is a localization factor and σ is the smooth parameter. Thus, the localization factor should be chosen such that $k \in [1,2]$ taking into account the noise amplitude and the accuracy expected for the localization edges. However, a proper trade-off between localization and noise reduction is reached when $k = 1$ [15]. This means that significant details and regions are still distinguishable by sharp edge when a Gaussian filter is applied ruled by parameter σ. By empirical procedure, a good selection of parameter σ is 3 or 4. Moreover, as $L = k\sigma$ with $k = 1$ and $\sigma \in [3,4]$ three or four levels of decomposition is a good choice.

In this sense, Harris operator analysis provides an objective way to determine the threshold. Thus, eigenvalues greater than zero are points of interest and the threshold is chosen based on this criteria. Moreover, gradient direction is also used to appraise the region borders.

3.3. Region Extraction and Postprocessing

Given each point of interest, by following the gradient direction the limits of the respective ROI can be reached as explained before. Then, defect centers are described by eigenvalues greater than zero in Harris matrix, while the size of defect is given by the number of steps necessary to find out a reduction in the gradient magnitude, i.e., whenever it holds that $\mathbf{\Delta}_{\Sigma}(\mathbf{k}) \geq \mathbf{\Delta}_{\Sigma}(\mathbf{k} \pm \mathbf{v})$. By using the introduced balanced error [16], we choose the size in opening and closing operation

to enhanced the ROI. In this sense, the results shows that a good compromise is made with, a 5x5 structuring element to closing and 3x3 structuring element to opening in morphological operation.

3.4. Evaluation Method

Evaluation of proposed methodology is carried out by using the commonly known data mining metrics of misclassification that are described as follows:

— *True Positive Rate* (TPR): Number of pixels correctly defined as edge pixels, that is, the hits. $TPR = \frac{\mathbf{X}(i,j) \in \mathbf{\Omega}_p}{size\{\mathbf{\Omega}_p\}}, \forall \quad i, j, p$

— *False Positive Rate* (FPR): Number of pixels erroneously defined as edge pixels or false alarms. $FPR = \frac{\mathbf{X}(i,j) \in \mathbf{\Omega}_p}{size\{\mathbf{\Omega}_p\}}, \forall \quad i, j, p$

— *Perfect segmentation distance*: Euclidean distance between the automatic segmentation and ideal segmentation $TPR = 1,\ FPR = 0$. $d = \sqrt{FPR^2 + (1-TPR)^2}$.

— *Balanced error*: Weighted sum of false positive and false negative rates, i.e., [16], $\varepsilon = \omega_1 FPR + \omega_2 FNR$, if assuming $\omega_1 = \omega_2 = 0.5$, then errors have same contribution.

Each thermogram sequence is segmented manually and the performance is measured using the discrepancy, which is based on the number of missegmented pixels [2], by using above introduced metrics over each image sequence. Attained values of mean and standard deviation μ±σ for the CFRP007 plate are shown in Table 1. These values are compared with isodata (iterative technique for threshold selection), multimodal (histogram shape-based method) and 2D histogram (Co-occurrence matrix threshold selection) segmentation procedures. The other samples results are discussed but not are shown in this paper.

Table 1. *Performance of considered algorithms in the CFRP007 plate*

	2D Histogram	Isodata	Multimodal	Proposed
TPR	0.76±0.36	0.78±0.11	0.79± 0.12	0.80± 0.11
FPR	0.65± 0.33	0.34± 0.01	0.37± 0.09	0.03±0.00
d	0.89± 0.09	0.42± 0.05	0.45± 0.08	0.21±0.10
ε	0.44± 0.04	0.28± 0.05	0.29±0.06	0.12±0.05

Table 1 shows the average results in the *CFRP007* sample within interval 81.9 to 630 ms after heating. The proposed methodology shows a higher TPR metric at least of 1% with respect to thresholding-based procedures. However, the proposed methodology has a lower FPR in 30% compared with other tested procedures in Table. Moreover, deviation $\sigma_{FPR} = 0$ shows a stable behaviour, since error is the same in every frame. On the other hand, the plate geometry causes a FPR increase in thresholding-based procedures since more distant regions from the camera lens are represented with less intensity [17]. This intensity loss is reflected in the low resolution of ROI that mixes background with defects. Besides, the histogram 1D and 2D have a large FPR.

4. DISCUSSION

Other segmentation techniques found in INDT were studied to compare the proposed meth**odology. However, the** performance obtained by applying the algorithms proposed in [2, 4, 5] are omitted because these procedures have a poor performance with the database used or are application dependent and have no generalization property. This may be explained by the non homogeneous heating produced by the infrared nondestructive material inspection.

Thus, the methodology proposed in [2] only segments in average the 8.75 % of the pixels belonging to defects. This is owed to the fact that this methodology enhances the gray level values and one hot spot can be masked by the non homogeneous heating or the noise in the image.

The segmentation of infrared images proposed by [4] is done for a specific application and this can not be extended to a different cases where defect geometry changes.

The algorithm proposed in [5], finds the centroids correctly but non homogeneous heating impairs the performance of the growing algorithm, because gray values in defects are close in the boundaries and the region growing stop is imprecise.

The methodology proposed in [16] is a local thresholding procedure and the local approach of 2D histogram is inappropriate for INDT image segmentation given the presence of non uniform heating. On the other hand, this technique needs at least 15 times more execution time than the proposed methodology to obtain the optimal threshold making the algorithm impractical for online applications. Moreover, the results of isodata and multimodal segmentation procedures [18, 19] respectively, show a good segmentation of defects, but only the proposed methodology can detect almost all the defects.

The results show that in average the number of defects detected by the proposed methodology exceeds single thresholding-based procedures in 10% for ISODATA, 17% for 2D histogram and 2% for multimodal thresholding. Moreover, FPR metric for proposed methodology is almost 11% less than thresholding-based procedures. Thus, the methodology has a good ROI selection ability since it is based on ROI localized approach and not on pixel values separation that is difficult to discern in thermal images. Besides, the proposed methodology reduces the distance to perfect segmentation at least in 18% compared to thresholding procedures showing a good balance between FPR and TPR.

Balanced error metric shows that thresholding-based procedures is 10% higher with respect to the proposed methodology, showing little robustness of those methodologies to frame and material change. On the other hand, the proposed methodology has stable metric values showing smaller standard deviation values than in the other procedures used for comparison. Finally, the proposed methodology shows robustness in the presence of non-uniform heating hence thermal contrast enhancement methods such as Differential Absolute Contrast (DAC) or corrected DAC with thermal quadrupoles [12] are not required. Besides, neither transformations such as Discrete Fourier Transform carried on in Pulse Phase Thermography [20] nor operations such as first and second derivatives executed in TSR [21] are required.

To measure the processing times of DAC, corrected DAC and TSR a experiment on sample *CFRP006* is carried out to analyze 993 frames, each of which with size 261x246. Processing times are 36.82, 189.42, 27.29, and 122.34, respectively (this times are normalized with respect to the processing time of proposed methodology, i.e., the proposed methodology has a processing time of 1). On the other hand, the proposed methodology can also be used in passive thermography where there is one thermal image available of the inspected object and the techniques previously mentioned are not useful.

5. CONCLUSIONS

A methodology using multi-resolution analysis for ROI extraction using the redundant wavelet transform was presented. This methodology provides an improvement in region growing compared to thresholding procedures by using the gradient direction. In addition, wavelet transform preserves spatial information and this property is used for ROI extraction. Besides, the proposed methodology is robust to non-uniform heating due to the information provided by the change of scale in multi-resolution analysis. The multi-resolution analysis is complemented by using Harris operator that describes gradient distribution in a neighborhood close to points of interest or defect centers. On the other hand, the proposed representation space gives sufficient information for the detection of local maxima, i.e., only the significant pixels are preserved. One of the greatest advantages of the multi-resolution analysis for ROI extraction is that features are entirely local since region growing is always done on gradient stopping criteria and thermal contrast enhancement is omitted simplifying the process and saving processing time. In the proposed methodology the number of wavelet decomposition levels is selected a priori without using segmentation. Nevertheless, it is necessary to find out the structuring element size in the opening and closing for morphological operation depending on type of material and defects size and shape. In spite of these advantages, the proposed methodology as well as the others tested, fails in the segmentation of aluminum specimen due to high thermal conductivity. As future work it is intended to extract regions of interest in uncontrolled environments with illumination changes and wheatear conditions by using the multi-resolution analysis.

6. ACKNOWLEDGMENTS

This research is partially supported within the framework of COLCIENCIAS research project (code 111942520795), Natural Science and Engineering Research Council of Canada (NSERC), the Canada Research Program (CRC): Multipolar Infrared Vision Canada Research Chair (MiViM) for permission to use the databases in active inspection of materials and the program COLCIENCIAS-CIAM (Inter-American Materials Collaboration) 2008 and the Foundation for Research and Science Promotion of Banco de la República de Colombia.

REFERENCES

[1] Fassani R. and Trevisan O., "Analytical Modeling of Multipass Welding Process with Distributed Heat Source," Society of Mechanical Sciences and Engineering Proceeding, Rio de Janeiro (Brazilian), vol. 25 N° 3, 2003.
[2] Heriansyah R. and S. A. R. Abu-Bakar, "Defect detection in thermal image for nondestructive evaluation of petrochemical equipments," NDT and E International, vol. 42 issue 3, p. 729-740, 2009.
[3] Plotnikov Y. A., Rajic N. and Winfree W. P., "Means of eliminating background effects for defect detection and visualization in infrared thermography", Optical Engineering, vol 39 issue 4, 2000.
[4] Usamentiaga R., García D. F. and Molleda J., "Automatic tuning for the segmentation of infrared images considering uncertain ground truth", Electronic Imaging, vol 18 issue 1, 2009.
[5] Maldague X., Krapez J.C. and Poussart D., "Thermographic Nondestructive Evaluation (NDE): An algorithm for automatic defect extraction in infrared images", IEEE Transactions on Systems, MAN, and Cybernetics, vol 20 N° 3, p. 722-725, 1990.
[6] Abdel-Qader I., Yohali S., Abudayyeh O. and Yehiab S., "Segmentation of thermal images for non-destructive evaluation of bridge decks", NDT and E International, vol. 41 issue 1, p. 395-405, 2008.
[7] Mallat S., "A Wavelet Tour of Signal Processing", Academic Press, 1999.
[8] Shensa M. J., "The discrete wavelet transform: wedding the Átrous and mallat algorithms", IEEE Trans Signal Process, vol. 40 N° 10, 1992.
[9] Hien T. D., Nakao Z. and Chen Y. W., "Robust RDWT-ICA based information hiding", Soft Computing - A Fusion of Foundations, Methodologies and Applications, vol. 10 N° 12, p. 1135-1144, 2006.
[10] Mikolajczyk K. and Schmid C., "An affine invariant interest point detector", Proceedings of the 7th European Conference on Computer Vision, Copenhagen, Denmark, vol. 60 N°1, 128-142, 2002.
[11] Harris C. and Stephens M., "A combined Corner and edge detector", *Proceedings of the 4th Alvey Vision Conference, p. 147-151, 1988.*
[12] Benítez H. D., Loaiza H., Caicedo E., Ibarra-Castanedo C., Bendada A. H. and Maldague X., "Defect characterization in infrared non-destructive testing with learning machines", NDT and E International, vol. 42 issue 7, 630-643, 2009.
[13] Nixon M. S. and Aguado A. S., "Feature Extraction and Image Processing", Butterworth-Heinemann, 2002.
[14] Jain R., Kasturi R. and Schunck B., "Machine Vision", MIT Press and Mc Graw Hill, 1995.
[15] Ducottet C., Fournel T. and Barat C., "Scale-adaptive detection and local characterization of edges based on wavelet transform", Signal Processing in communications, vol 84 issue 11, 2115-2137, 2004.
[16] Feng D., Wenkang S., Liangzhou C., Yong D. and Zhenfu Z., "Infrared image segmentation with 2-D maximum entropy method based on particle swarm optimization (PSO)", Pattern Recognition Letters, vol. 26 issue 5, p.597-603, 2005.
[17] Kaplan H., "Practical Applications of Infrared Thermal Sensing and Imaging Equipment", SPIE - The International Society for Optical Engineering, 2007.
[18] Dianat R. and Kasaei S., "On Automatic Threshold Selection in Regression Method for Change Detection in Remote Sensing Images", The 4th International Symposium on Telecommunications, Tehran, Iran, 2008.
[19] Sezgin M. and Sankur B., "Survey over image thresholding techniques and quantitative performance evaluation", Journal of Electronic Imaging, vol. 13 N°146, 2004.
[20] C. Ibarra-Castanedo C. and Maldague X., "Interactive Methodology for Optimized Defect Characterization by Quantitative Pulsed Phase Thermography", Research in NonDestructive Evaluation, vol. 16 issue 4, p. 175-193, 2005.
[21] Shepard S. M., "Advances in Pulsed Thermography", SPIE, Thermosense XXIII, 2001.